Volume 12 | Number 11 | 21 March 2016 | Pages 2807–2978

Soft Matter

www.softmatter.org

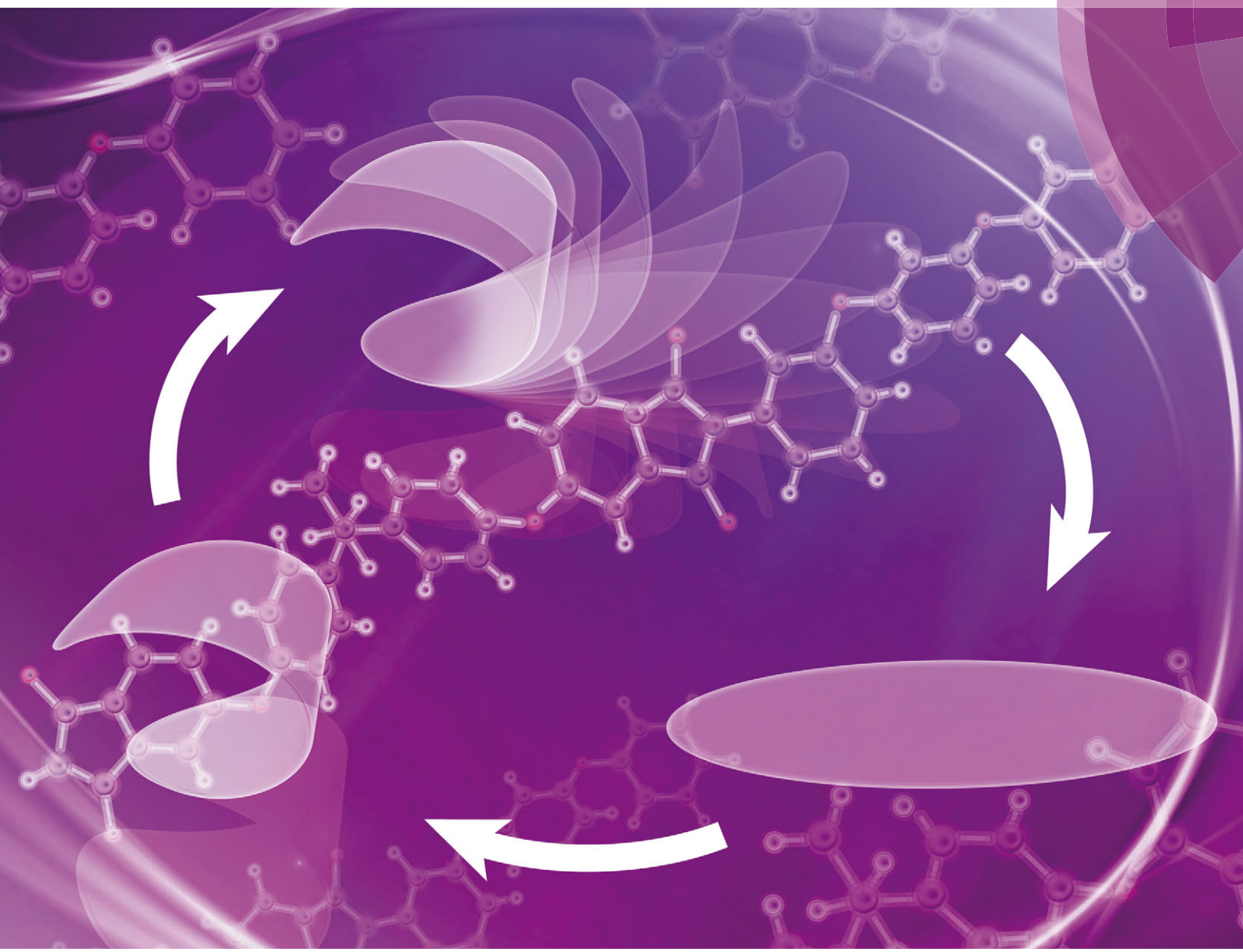

ISSN 1744-683X

ROYAL SOCIETY OF CHEMISTRY

PAPER
Jinsong Leng *et al.*
Optically transparent high temperature shape memory polymers

Soft Matter

PAPER

Cite this: *Soft Matter*, 2016, 12, 2894

Optically transparent high temperature shape memory polymers†

Xinli Xiao,[ab] Xueying Qiu,[a] Deyan Kong,[a] Wenbo Zhang,[a] Yanju Liu[c] and Jinsong Leng*[b]

Received 3rd November 2015,
Accepted 9th December 2015

DOI: 10.1039/c5sm02703a

www.rsc.org/softmatter

Optically transparent shape memory polymers (SMPs) have potential in advanced optoelectronic and other common shape memory applications, and here optically transparent shape memory polyimide is reported for the first time. The polyimide possesses a glass transition temperature (T_g) of 171 °C, higher than the T_g of other transparent SMPs reported, and the influence of molecular structure on T_g is discussed. The 120 μm thick polyimide film exhibits transmittance higher than 81% in 450–800 nm, and the possible mechanism of its high transparency is analyzed, which will benefit further research on other transparent high temperature SMPs. The transparent polyimide showed excellent thermomechanical properties and shape memory performances, and retained high optical transparency after many shape memory cycles.

1 Introduction

With the rapid development of optoelectronics, transparent polymers have attracted more and more attention for their application in both academic and engineering fields due to their superior flexibility, lightness and processability compared with the fragile glass analogues.[1–6] Shape memory polymers (SMPs) are smart polymers that can remember their deformed temporary shapes and then recover to their original shape under external stimuli.[7–12] SMPs have been used as biomedical devices,[13–16] smart fabrics,[17] deployable structures,[18] actuators,[19] *etc.*[20,21] The optically transparent SMPs exhibit shape memory effects besides their optical transparency, which will produce some unusual properties. For example, the deformable and adaptive optics made of transparent shape memory poly(ethylene-*co*-vinyl acetate) (PEVA) can produce real-time optimum device performances, and the phase transition temperature (melting temperature) of PEVA is 63 °C.[22] Similar to other conventional optically transparent SMPs such as polyester (T_g: ~78 °C) and polystyrene (T_g: ~100 °C), their optical and mechanical properties will be deteriorated at high temperatures.[22–25] Thus the optically transparent polymers with high thermal resistance are greatly desired due to the ever-increasing demands for high reliability and high integration in optoelectronic devices.[3,5] Accordingly, the optically transparent high temperature SMPs are expected to have potential in advanced adaptive optoelectronic applications. However, to date there is no report on highly transparent SMPs with T_g higher than 120 °C.[22–28]

Polyimides are high performance polymers due to their high thermal stabilities, excellent mechanical properties and low dielectric constants, and they are good candidates for various fields, including aerospace, automobile, microelectronic and optoelectronic applications.[3,4] The conventional aromatic polyimide films generally possess intense deep colors and poor optical transparency due to the formation of strong intra-/inter-molecular charge transfer complex (CTC) interactions, which greatly limits their application in areas where high transparency is the basic need.[1–3] Conversely, highly transparent polyimides are of special importance for optoelectronic applications such as transparent flexible substrates in displays, flexible printing circuit boards, optical waveguides for communication interconnects, and optical half-waveplates for planar lightwave circuits.[4–6] The addition of shape memory effects to the optically transparent polyimide will expand their application enormously. Moreover, the transparent shape memory polyimide is also promising in common shape memory applications that it will undergo in high temperature environments, such as deployable space structures, jet propulsion systems, high temperature sensors and actuators.[29,30] To date, although there are several reports on yellow or brown shape memory polyimides, there is no report on highly transparent shape memory polyimide.[31–33]

[a] *Department of Chemistry, Harbin Institute of Technology, No. 92 West Dazhi Street, Harbin 150001, People's Republic of China*
[b] *Centre for Composite Materials and Structures, Harbin Institute of Technology, No. 2 Yikuang Street, Harbin 150080, People's Republic of China. E-mail: lengjs@hit.edu.cn*
[c] *Department of Astronautical Science and Mechanics, Harbin Institute of Technology, No. 92 West Dazhi Street, Harbin 150001, People's Republic of China*

† Electronic supplementary information (ESI) available: Molecular weight, IR, XRD, optical photograph, UV-Vis transmittance, DMA, TGA of other less transparent shape memory polyimides, IR spectra of poly(amic acid) (PAA), UV-Vis transmittance of TSMPI films with different thicknesses, three-dimensional structures of the polyimide chains with different molecular weights, molecular structures of the reported shape memory polyimides, and the video showing deployable shape recovery process of TSMPI are shown in the ESI. See DOI: 10.1039/c5sm02703a

In the past few decades, many efforts have been made to develop highly transparent low-colored and colorless polyimides by suppressing CTC interactions, such as incorporation of unsymmetrical or bulky pendant units,[34] introduction of a strong electron-withdrawing fluorinated or sulfone group,[35] and adoption of alicyclic moieties in the polymer structures.[36] However, most of the above mentioned transparent polyimides demand expensive or intricate reactants.[34–36] In the current report, by employing flexible bis phenol A dianhydride (BPADA) as dianhydride and flexible 1,3-bis(3-aminophenoxy)benzene (BAB) as diamine, as well as controlling the molecular weight, highly transparent shape memory polyimides are obtained for the first time.

The polyimide exhibits T_g higher than those of other transparent SMPs, and the relationship between molecular structure and T_g is analyzed, and the possible mechanism of its transparency is discussed. The highly transparent polyimide possesses excellent shape memory performances and stable optical properties, which guarantee its potential in recyclable applications.

2 Experimental

2.1 Synthesis of the transparent shape memory polyimide

BPADA (>98%) was purchased from TCI and BAB (98%) was purchased from Sigma-Aldrich Co., and the monomers were used as received. Dimethylacetamide (DMAc) was purchased from Kemiou Chemical Reagent Co. Ltd and distilled using activated 4 Å molecular sieves under reduced pressure.

4.55 mmol BAB and 20 ml DMAc were added to a three-necked flask and then stirred under dry nitrogen for 20 min. 5 mmol BPADA was fed into the flask in batches within 1 h, and intense mechanical stirring was executed at room temperature for 22 h to form viscous poly(amic acid) (PAA). The flask was transferred into a vacuum drying chamber and heated under vacuum at 30 °C for 3 h to remove the bubbles. Thin iron sheets were used as back-up to make sure that the glass substrate is horizontal, as determined by an air-bubble level. The PAA was poured onto the glass substrate and underwent a step-wise imidization curing process at 80 °C/2 h, 110 °C/2 h, 160 °C/2 h, 190 °C/2 h and 230 °C/1 h. The polyimide was detached away from glass in deionized water, and heated at 120 °C for 5 h to remove the water. Other less transparent shape memory polyimide samples with different properties were synthesized with different molar ratios of BPADA to BAB, as shown in the ESI† (Table S1).

2.2 Molecular weight and structural characterization

Molecular weights of polyimide samples were determined by size exclusion chromatography (SEC) using waters 2414 equipped with a refractive index detector with dimethylformamide (DMF) as an eluent at 35 °C, and the molecular weight *versus* evolution time was calculated using narrow polydispersity poly(styrene) standards.

The Fourier transform infrared (FT-IR) spectra of the polyimide samples were registered on Thermo Nicolet Nexus 870 from 650 to 4000 cm^{-1} at a resolution of 4 cm^{-1}. X-ray diffraction (XRD) was carried out on Rigaku Miniflex 600 under Cu Kα radiation (λ = 0.15405 nm), and the accelerating voltage and emission current were 40 kV and 50 mA, respectively.

2.3 Optical properties characterization

The ultraviolet-visible (UV-Vis) transmittance of the transparent shape memory polyimide film was executed using a Perkin Elmer Lambda 1050 UV/Vis/NIR spectrometer from 200 to 800 nm at a resolution of 1 nm. Three tests were conducted for per sample with each exhibiting consistent results, and only one transmittance spectrum is shown for clarity.

2.4 Thermomechanical and thermal properties characterization

Storage modulus and loss factor of the specimens *versus* temperature were characterized by dynamic mechanical analysis (DMA) on Netzsch Q800. DMA tests were conducted in the tensile mode at the frequency of 1 Hz with a heating rate of 3 °C min^{-1} on slabs with the dimension of 38 mm × 3 mm × 0.12 mm. The thickness of the slab was the thickness of the film measured, and only the samples with uniform thickness were chosen for DMA analysis. Three tests were conducted for per sample with each exhibiting the consistent results, and only one DMA spectrum is shown for clarity.

Differential scanning calorimetry (DSC) was used to characterize the thermal properties of the polymers at a heating rate of 10 °C min^{-1} using NETZSCH STA 449C. The thermal stability of the polyimide was characterized by thermal gravimetric analysis (TGA) under a N_2 environment on a Mettler-Toledo TGA/DSC instrument at a heating rate of 10 °C min^{-1}.

2.5 Shape memory characterization

The deployable shape memory process of the polyimide was tested with a round sheet. The polyimide sheet was rolled on the surface of the hot stage and the deformed shape was fixed by removal from the hot stage to room temperature. Then the sample recovered to its original shape when it was placed back to the hot stage, and the shape recovery process was recorded using a digital video (Canon VIXIA HF R500).

The stretchable shape memory performance was executed with consecutive stretch–contraction processes using the controlled force mode on TA INSTUMENT Q800. The steps are carried out as follows: (a) heating a sample to T_g + 20 °C, (b) applying a force that would prolong the sample; (c) reducing to T_g − 40 °C, (d) force removal, (e) heating to T_g + 20 °C. Once the sample recovered to a constant value, the process was repeated by applying the same force used in step (b).

3 Results and discussions

3.1 Molecular weight and structures

The polycondensation process of the highly transparent shape memory polyimide (TSMPI) is shown in Scheme 1. The highly TSMPI possesses a number average molecular weight (M_n) of

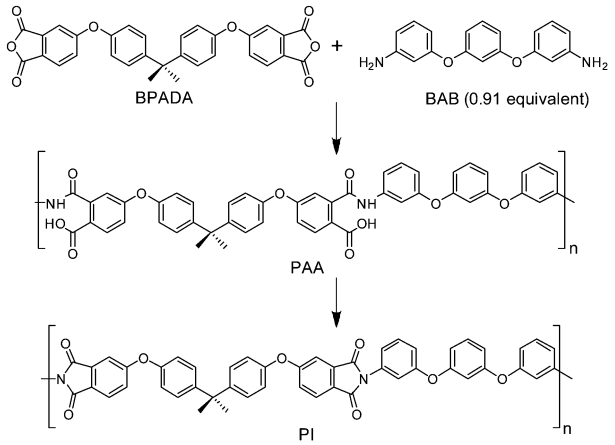

Scheme 1 Polycondensation of the highly transparent shape memory polyimide.

21.7 kg mol^{-1} and a weight average molecular weight (M_w) of 42.5 kg mol^{-1}. The polyimide samples with higher M_n are less transparent than the almost colorless polyimide, while the samples with lower M_n don't possess shape memory effects, as summarized in the ESI† (Table S1).

The representative section of IR spectra (800–2000 cm^{-1}) of TSMPI is shown in Fig. 1a, and the peaks at around 1780 cm^{-1} (asymmetric stretching of C═O), 1718 cm^{-1} (symmetric stretching of C═O) and 1373 cm^{-1} (stretching vibration of C–N–C) confirm the formation of imides. There is no evidence of carbonyl peaks of isoimide in 1795–1820 or 921–934 cm^{-1}, indicating the absence of isoimides. The carbonyl stretching in an inter-molecular imide linkage near 1670 cm^{-1} is not observed either.[38] These results demonstrate that the sample is fully imidized within the detection limit of IR. The typical IR peaks of PAA disappeared and the characteristic peaks of polyimide appeared after thermal curing, as manifested in the ESI† (Fig. S1), and the IR spectra of other less transparent shape memory polyimides are shown in the ESI† (Fig. S2).

The wide-angle X-ray diffraction pattern of TSMPI is shown in Fig. 1b, and it displays a broad peak centered at about 18° due to the diffraction of intermolecular packing, characteristic of some regularity combined with amorphous halo.[34] The XRD results manifest that the polyimide is amorphous in morphological structures, mainly due to loose chain packing and aggregation caused by the ether and isopropylidene linkages in dianhydride, as well as the *meta*-substituted ether linkages in the diamine units. The XRD spectra of other less transparent polyimide samples are shown in the ESI† (Fig. S3).

3.2 Optical transparency

The optical properties of the polyimide were evaluated by both UV-Vis spectra and their physical appearance. As illustrated in Fig. 2, the 120 μm thick TSMPI film shows very good optical transparency, its cut-off wavelength value (λ_0) is 381 nm, and the transmittance at 450 and 500 nm is 82% and 85%, respectively. Optical photographs of the TSMPI film are shown in the inlet, and it is observed that the highly transparent TSMPI is almost colorless. The thickness of the film can affect its optical properties, and the UV-Vis spectra of the TSMPI film with different thicknesses are shown in the ESI† (Fig. S4). A thicker film will lead to less transparency, and the transmittance at 450 nm for films with thicknesses of 120, 180, 260 and 320 μm is 82%, 79%, 75% and 71%, respectively. The UV-Vis spectra of other less transparent shape memory polyimide samples are shown in the ESI† (Fig. S5), and their cut-off wavelength values and transmittance are summarized in the ESI† (Table S2).

It has been proved that the coloration of aromatic PIs is mainly caused by the intra-/inter-molecular charge transfer complex (CTC) formation between the alternating electron–acceptor (dianhydride) and electron–donor (diamine) moieties, and higher CTC interactions lead to deeper colors.[1,3,5] In this regard, the high transparency of TSMPI originates from the strongly suppressed CTC interactions, and the 3-dimensional (3D) molecular structure of TSMPI is shown in Fig. 3.

As can be observed from Fig. 3a, the introduction of large pendant isopropyl groups in the dianhydride will increase the free volume of each molecule and destroy the compact stacking of molecular chains, thus decreasing the intermolecular CTC interactions. The isopropyl groups and the flexible ether linkage in the dianhydride can hinder the charge flow along the main chains, which will suppress the intramolecular CTC interactions. The molecular structure is folded when

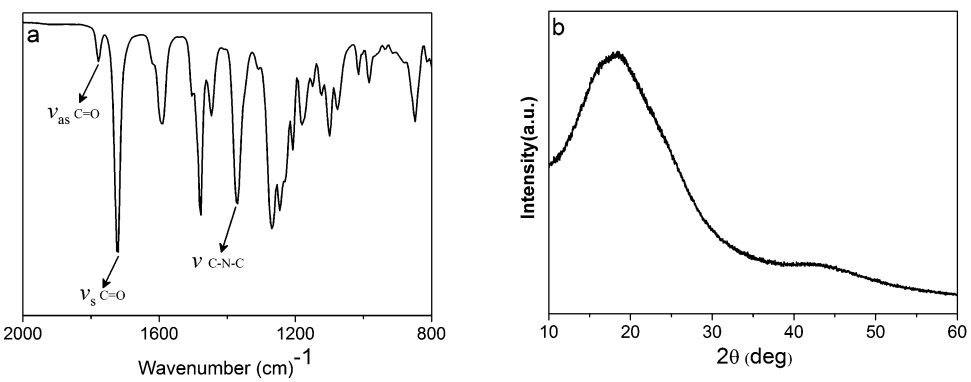

Fig. 1 FT-IR (a) and XRD (b) spectra of TSMPI.

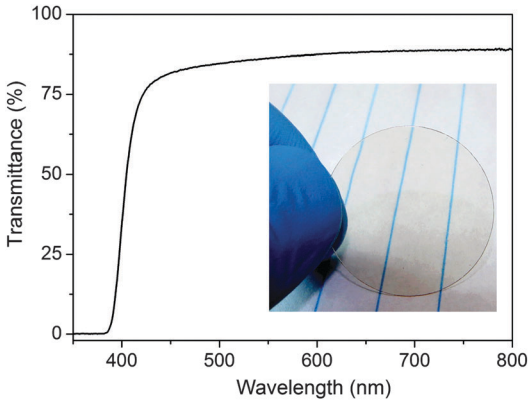

Fig. 2 UV-Vis spectra of a 120 μm thick TSMPI film, and the inlet shows its optical photograph.

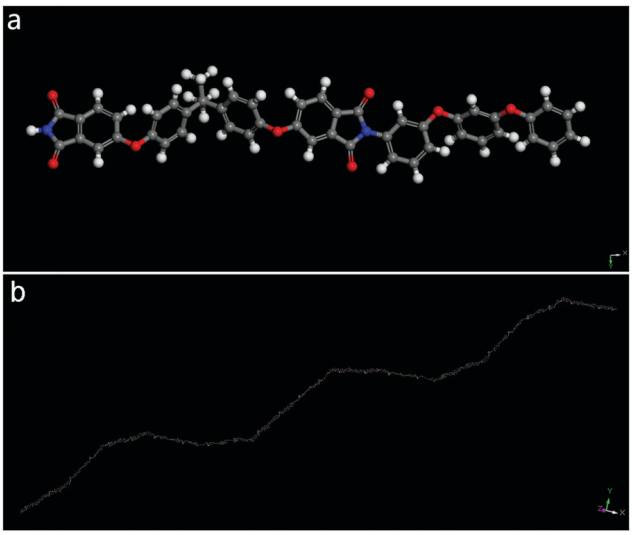

Fig. 3 Three-dimensional structures of structural unit (a) and polyimide chain (b) of TSMPI. The grey, white, red and blue of molecular structure display C, H, O and N, respectively.

meta-substituted, and the intermolecular CTC interactions decrease. Both the *meta*-substituted structures and the flexible ether linkage in the diamine can decrease charge flow, which will reduce the intramolecular CTC interactions. Consequently, the formation of both inter- and intra-molecular CTC interactions is obstructed. It is well-known that the intermolecular interactions of polymers will become weaker for samples with lower M_n, thus colors of the polyimide samples get lighter and lighter with the decrease of M_n and TSMPI becomes almost colorless, as shown in the ESI† (Fig. S6). Judged from M_n (21.7 kg mol^{-1}) and the structural unit (807 g mol^{-1}), a typical TSMPI molecular chain comprises 27 structural units, and its characteristic folded 3D molecular structure is shown in Fig. 3b. But the polyimide samples with M_n lower than that of TSMPI can't produce good shape memory effects, indicating that chain entanglements are essential for the shape memory process of thermoplastic polyimide.[12,30,31] The folded long chains are apt to form chain entanglements, and the molecular chains of samples with lower M_n are less folded, as illustrated by their 3D structures in the ESI† (Fig. S7).

The development of transparent PI has been negatively affected by the high cost of commercially available monomers, as the cost of transparent PI films is largely determined by the monomers.[39] Most of the reported highly transparent polyimide samples are synthesized using intricate and expensive reagents, and some typical monomers for transparent PIs, such as 1,2,3,4-cyclobutane tetracarboxylic dianhydride (5 g/1850 CNY),[40,41] 3,4-dicarboxy-1,2,3,4-tetrahydro-1-naphthalene succinic dianhydride (5 g/690 CNY),[37,40] and 2,2′-bis(3,4-dicarboxyphenyl) hexafluoro-propane dianhydride (5 g/1990 CNY) are rather expensive.[40,42] Compared with them, the 2,2-bis[4-(3,4-dicarboxyphenoxy)phenyl]propane dianhydride (25 g/790 CNY) used in this report is relatively cheap. Some other monomers for transparent PIs such as 9,9-bis[4-(4-amino-2-trifluoromethylphenoxy)phenyl]-fluorene,[39] 1,4-bis[4-amino-2-trifluoromethylphenoxy]-2,5-di-tert-butylbenzene,[43] and 2,2′-bis[4-(3-nitro-5-trifluoromethylphenoxy)-phenyl]sulfone are synthesized in the authors' own lab by intricate ways,[34] and they are not commercially available. Here we offered an economical way to obtain optically transparent polyimide with common reactants.[40] TSMPI can be dissolved in DMF, DMAc and NMP, and the solubility can be explored to produce films at low temperature, avoiding the possible damages to optoelectronic devices caused by high temperature.[4,34]

3.3 Thermomechanical and thermal properties

The thermomechanical properties of TSMPI are analyzed by DMA, as shown in Fig. 4. It is observed that the tensile storage modulus (E') decreases slowly with the increase of temperatures in glassy state, but there is an essential decrease around T_g, and the storage modulus of TSMPI at 50 °C, 151 °C (T_g − 20 °C) and 191 °C (T_g + 20 °C) are 2.2 GPa, 1.7 GPa and 4.1 MPa, respectively.

The peak of the loss factor (tan δ) obtained by DMA is often taken as T_g of rigid-chain polymers, and TSMPI exhibits T_g of 171 °C, which is higher than those of other transparent SMPs, but lower than those of shape memory polyimides. It has been proved that the relative flexibility of the polymer backbone can affect dynamics through the glass transition,[44] which has great

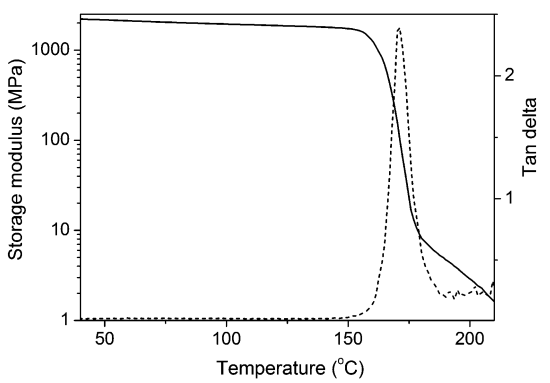

Fig. 4 Tensile storage modulus (solid line) and loss factor (dotted line) *versus* temperature of the TSMPI.

influence on T_g of polymers. Many SMPs composed of polymers with flexible main chains possess T_g lower than 110 °C, while high temperature SMPs, such as polyimide, polycyanate and poly(ether ether ketone)ionomers, are composed of rigid main chains comprising phenyl rings and flexible linkages.[8,32,37] Shape memory polyimides are obtained from the polycondensation of dianhydride and diamine, and the TSMPI in this report is obtained from BAB and BPADA. The isopropylidene and ether linkages within the backbone, together with the meta-substitute structure provide flexibility to the rigid polyimide molecule, and the molecular chains act as a reversible phase of the shape memory process. The shape memory polyimide samples obtained from the polycondensation of BPADA/2,2-bis[4-4(-aminophenoxy)phenyl]propane (BAPP), 4,4′-(hexafluoroisopropylidene) diphthalic anhydride (6FDA)/BAB and 4,4′-oxydiphthalic dianhydride (ODPA)/4,4′-diaminodiphenyl ether (ODA) exhibited T_g of 212 °C, 222 °C and 261 °C, respectively.[31,32,45] The molecular structures of the typical shape memory polyimide samples are illustrated in the ESI† (Fig. S8). For the dianhydrides of shape memory polyimides, BPADA possesses one isopropylidene and two ether linkages, 6FDA possesses one hexafluoroisopropylidene, and ODPA possesses one ether linkage on the backbone. Among them, BPADA is the most flexible dianhydride. For the diamines, BAPP possesses an isopropylidene and two ether linkages in a highly symmetrical manner, BAB possesses two meta-substituted ether linkages, and ODA possesses one ether linkage in the backbone. Among them, BAB is the most flexible diamine. From the standpoint of molecular structures, it is obvious that the main-chain flexibility of different types of shape memory polyimide samples are arranged in the sequence of BPADA/BAB > BPADA/BAPP > 6FDA/BAB > ODPA/ODA. As a result, the polyimide of BPADA/BAB exhibits T_g lower than those of the previously reported shape memory polyimides. The modulus and tan δ of other less transparent shape memory polyimides are shown in the ESI† (Fig. S9).

The thermal stability of the TSMPI is examined by TGA, and the weight loss and the derivative of weight are shown in Fig. 5. The major decomposition was observed by examining the derivative of the weight curves, and the sample shows high thermal stability with minimal decomposition (<5%) to 485 °C before major decomposition beginning at 540 °C. The pyrolysis left about 46% carbonaceous char at 800 °C, and these results indicate that TSMPIs are thermally stable. The TGA spectra of other less transparent shape memory polyimide samples are shown in the ESI† (Fig. S10).

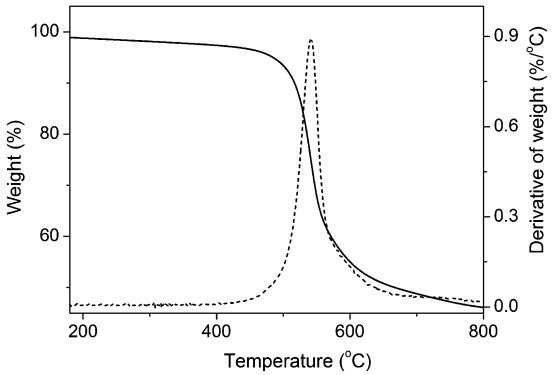

Fig. 5 TGA spectra of the weight loss (solid line) and derivative of weight (dashed line) of TSMPI.

3.4 Shape memory properties

Deployable application is the commonly used pattern of SMPs, and the shape memory properties are studied using a round polyimide sheet. The sheet was rolled on a hot stage, and the temporary shape was fixed by cooling to room temperature. Then the sample recovered to its original shape when it was placed back to the same hot-stage. The typical images showing the deformed shape and the consequent shape recovery process of SMTPI5 are shown in Fig. 6, and the movie is in the ESI† (Movie S1). The process is repeated thirty times with no damage observed, and every time it appears to recover completely to the initial shape.

Stretchable application is another commonly used pattern, and it is also usually employed to determine shape recovery (R_r) and shape fixity (R_f) of SMPs. R_r and R_f are two important factors in determining shape memory performances of the SMP, which represents the capability of the SMP to recover to its original shape and maintain the mechanical deformation, respectively. R_r is calculated using eqn (1).

$$R_r(N) = \frac{\varepsilon_m(N) - \varepsilon_p(N)}{\varepsilon_m(N) - \varepsilon_p(N-1)} \times 100\% \quad (1)$$

where ε_m, ε_p and N denote the strain after the stretching step (before cooling), the strain after recovery, and the cycle number, respectively. R_f is calculated using eqn (2).

$$R_f(N) = \frac{\varepsilon_u(N)}{\varepsilon_m(N)} \times 100\% \quad (2)$$

where ε_u denotes the strain in the fixed temporary shape. The stretchable pattern was examined with consecutive stretch-contraction cycles, and the cycles of TSMPI are shown in Fig. 7.

It is observed that R_f of the first, second and third cycle is 99.2%, 99.3% and 99.2%, respectively, consistent from one cycle to another. However, R_r is 80.1% for the first cycle, 97.6% and 97.0% for the second and third cycle. The difference in R_r between the first and the following cycles is generally

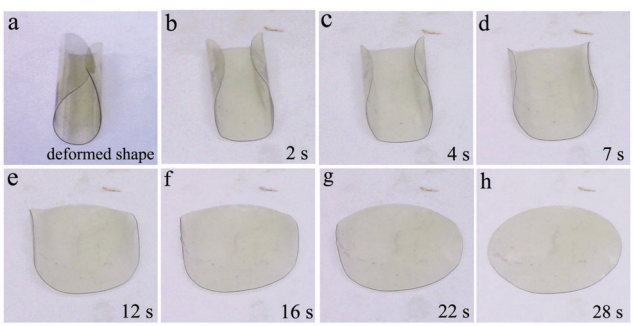

Fig. 6 Deployable shape memory pattern of TSMPI. (a) Deformed temporary shape and (b)–(h) shape recovery process of TSMPI on a 190 °C hot-stage, and the subscripts indicate the time on the hot-stage.

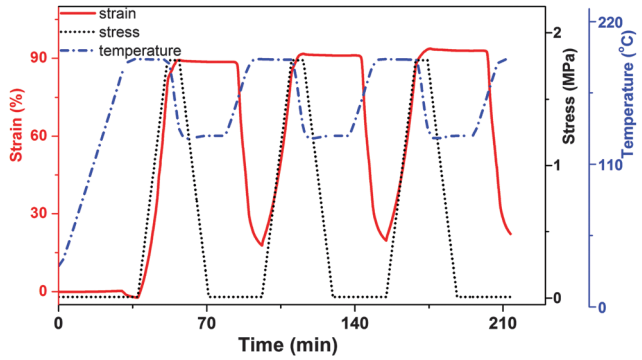

Fig. 7 The stretchable shape memory process of TSMPI with two-dimensional demonstration of changes in strain, stress and temperature *versus* time.

ascribed to the residual strain resulting from the processing history.[46] TSMPI possesses excellent shape memory properties, mainly due to the large difference in the storage modulus in glassy and rubbery states.[8,47] The high storage modulus in the glassy state originates from the potential elasticity, and the low storage modulus in the rubbery state is caused by the entropy elasticity due to micro-Brownian movement.

3.5 Optical stability

The stable optical properties of TSMPI are of great importance for their applications, as they may be exposed not only to disposable but also to recyclable devices. Here the optical stability is characterized by the transmittance of the sample after 5, 10, 15, 20 and 30 shape memory cycles, as shown in Fig. 8.

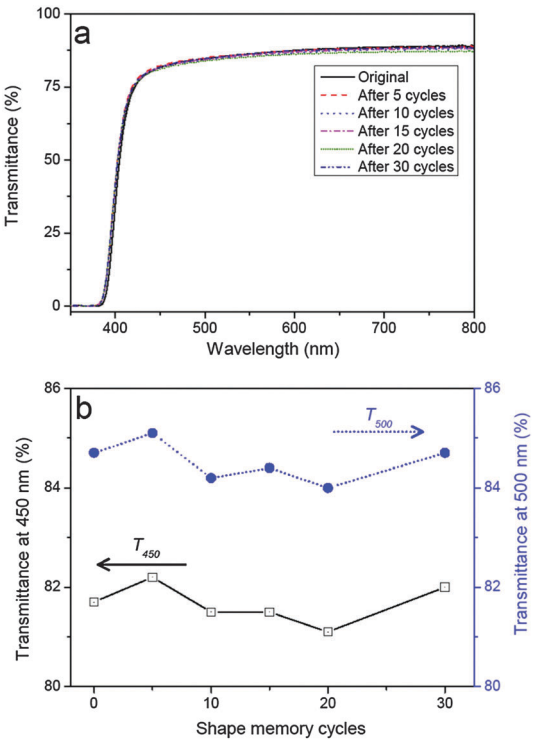

Fig. 8 Optical properties of TSMPI exposed to shape memory cycles. (a) Transmittance before and after 5, 10, 15, 20 and 30 shape memory cycles at 350–800 nm. (b) Particular transmittance values at 450 and 500 nm after different cycles.

It is observed in Fig. 8a that there is almost no discernable difference in transmittance. The particular transmittance values at 450 and 500 nm are shown in Fig. 8b, and there is no trend of degradation within the characterized shape memory cycles. These results indicate that TSMPI possesses stable optical properties, which will benefit their applications as recyclable optoelectronic devices.

4 Conclusion

In summary, this report has offered an efficient way to obtain optically transparent shape memory polyimides that have vast potential in controlling the chemical structure and the molecular weight. The high optical transparency mainly originates from the suppressed intra-/inter molecular charge transfer complex interactions caused by the special structure of the polyimide. The transparent shape memory polyimide shows T_g of 171 °C, higher than those of other optically transparent SMPs. The transparent polyimide exhibits excellent shape memory properties, and it retains the stable optical transparency after shape memory cycles. The combination of unusual optical properties with shape memory effects guarantees its foreseeable applications in advanced optoelectronic devices and other high temperature applications.

Conflict of interest

The authors declare no competing financial interests.

Acknowledgements

This research was financially supported by National Natural Science Foundation of China (Granted No. 51402073, 11225211 and 11272106), China Postdoctoral Science Foundation (Granted No. 2013M531030), and Fundamental Research Funds for the Central Universities (Grant No. HIT. NSRIF. 2011018 and HIT. NSRIF. 2012064).

References

1 K. Mizoguchi, Y. Shibasaki and M. Ueda, *J. Photopolym. Sci. Technol.*, 2007, **20**, 181–186.
2 J. M. Liu, T. M. Lee, C. H. Wen and C. M. Leu, *J. Soc. Inf. Disp.*, 2011, **19**, 63–69.
3 M. C. Choi, J. C. Hwang, C. Kim, S. Ando and C. S. Ha, *J. Polym. Sci., Part A: Polym. Chem.*, 2010, **48**, 1806–1814.
4 K. Takizawa, J. Wakita, S. Azami and S. Ando, *Macromolecules*, 2011, **44**, 349–359.
5 C. P. Yang and Y. Y. Su, *Polymer*, 2005, **46**, 5797–5807.
6 J. C. Kim and J. H. Chang, *Macromol. Res.*, 2014, **22**, 1178–1182.

7 G. Tandon, K. Goecke, K. Cable and J. Baur, *J. Intell. Mater. Syst. Struct.*, 2009, **20**, 2127–2143.
8 I. A. Rousseau, *Polym. Eng. Sci.*, 2008, **48**, 2075–2089.
9 F. Pilate, R. Mincheva, J. D. Winter, P. Gerbaux, L. Wu, R. Todd, J. M. Raquez and P. Dubois, *Chem. Mater.*, 2014, **26**, 5860–5867.
10 X. D. Jin, Q. Q. Ni and T. Natsuki, *J. Compos. Mater.*, 2011, **45**, 2547–2554.
11 M. Behl, M. Y. Razzaq and A. Lendlein, *Adv. Mater.*, 2010, **22**, 3388–3410.
12 X. L. Xiao, D. Y. Kong, X. Y. Qiu, W. B. Zhang, Y. J. Liu, S. Zhang, F. H. Zhang, Y. Hu and J. S. Leng, *Sci. Rep.*, 2015, **5**, 14137.
13 K. Yu, Q. Ge and H. J. Qi, *Nat. Commun.*, 2014, **5**, 3066.
14 C. M. Yakacki, R. Shandas, C. Lanning, B. Rech, A. Eckstein and K. Gall, *Biomaterials*, 2007, **28**, 2255–2263.
15 K. Nagahama, Y. Ueda, T. Ouchi and Y. Ohya, *Biomacromolecules*, 2009, **10**, 1789–1794.
16 H. Chen, Y. Li, Y. Liu, T. Gong, L. Wang and S. Zhou, *Polym. Chem.*, 2014, **5**, 5168–5174.
17 J. Hu, Y. Zhu, H. Huang and J. Lu, *Prog. Polym. Sci.*, 2012, **37**, 1720–1763.
18 W. M. Sokolowski and S. C. Tan, *J. Spacecr. Rockets*, 2007, **44**, 750–754.
19 Y. P. Liu, K. Gall, M. L. Dunn, A. R. Greenberg and J. Diani, *Int. J. Plast.*, 2006, **22**, 279–313.
20 K. Kratz, S. A. Madbouly, W. Wagermaier and A. Lendlein, *Adv. Mater.*, 2011, **23**, 4058–4062.
21 Y. Y. Zhang, Y. M. Li and W. G. Liu, *Adv. Funct. Mater.*, 2015, **25**, 471–480.
22 H. X. Xu, C. J. Yu, S. D. Wang, V. Malyarchuk, T. Xie and J. A. Rogers, *Adv. Funct. Mater.*, 2013, **23**, 3299–3306.
23 C. S. Zhang, Q. Q. Ni, S. Y. Fu and K. Kurashiki, *Compos. Sci. Technol.*, 2007, **67**, 2973–2980.
24 H. G. Jeon, P. T. Mather and T. S. Haddad, *Polym. Int.*, 2000, **49**, 453–457.
25 T. F. Scott, R. B. Draughon and C. N. Bowman, *Adv. Mater.*, 2006, **18**, 2128–2132.
26 J. M. Haberl, A. Sánchez-Ferrer, A. M. Mihut, H. Dietsch, A. M. Hirt and R. Mezzenga, *Adv. Funct. Mater.*, 2014, **24**, 3179–3186.
27 J. J. Song, H. H. Chang and H. E. Naguib, *Polymer*, 2015, **56**, 82–92.
28 A. Khaldi, J. A. Elliott and S. K. Smoukov, *J. Mater. Chem. C*, 2014, **2**, 8029–8034.
29 Y. Shi and R. A. Weiss, *Macromolecules*, 2014, **47**, 1732–1740.
30 X. L. Xiao, D. Y. Kong, X. Y. Qiu, W. B. Zhang, F. H. Zhang, L. W. Liu, Y. J. Liu, S. Zhang, Y. Hu and J. S. Leng, *Macromolecules*, 2015, **48**, 3582–3589.
31 M. Yoonessi, Y. Shi, D. A. Scheiman, M. Lebron-Colon, D. M. Tigelaar, R. A. Weiss and M. A. Meador, *ACS Nano*, 2012, **6**, 7644–7655.
32 H. Koerner, R. J. Strong, M. L. Smith, D. H. Wang, L. S. Tan, K. M. Lee, T. J. White and R. A. Vaia, *Polymer*, 2013, **54**, 391–402.
33 J. A. Shumaker, A. J. W. McClung and J. W. Baur, *Polymer*, 2012, **53**, 4637–4642.
34 L. Zhai, S. Y. Yang and L. Fan, *Polymer*, 2012, **53**, 3529–3539.
35 Y. M. Kim and J. H. Chang, *Macromol. Res.*, 2013, **21**, 228–233.
36 H. Masatoshi, F. Mari, I. Junichi, Y. Shinya, T. Eiichiro, K. Takashi and I. Atsushi, *Polymer*, 2014, **55**, 4693–4708.
37 H. J. Ni, J. G. Liu, Z. H. Wang and S. Y. Yang, *J. Ind. Eng. Chem.*, 2015, **28**, 16–27.
38 C. A. Pryde, *J. Polym. Sci. Part A: Polym. Chem.*, 1989, **27**, 711–724.
39 C. P. Yang, Y. Y. Su and Y. C. Chen, *Eur. Polym. J.*, 2006, **42**, 721–732.
40 Websites of Tokyo Chemical Industry, http://www.tcichemicals.com/zh/cn/product/index.html.
41 H. Suzuki, T. Abe, K. Takaishi, M. Narita and F. Hamada, *J. Polym. Sci., Part A: Polym. Chem.*, 2000, **38**, 108–116.
42 T. L. Li and S. L. C. Hsu, *Eur. Polym. J.*, 2007, **43**, 3368–3373.
43 C. P. Yang and F. Z. Hsiao, *J. Polym. Sci., Part A: Polym. Chem.*, 2004, **42**, 2272–2284.
44 J. D. Merline, N. C. P. Reghunadhan, C. Gouri, G. G. Bandyopadhyay and K. N. Ninan, *J. Appl. Polym. Sci.*, 2008, **107**, 4082–4092.
45 Q. H. Wang, Y. K. Bai, Y. Chen, J. P. Ju, F. Zheng and T. M. Wang, *J. Mater. Chem. A*, 2015, **3**, 352–359.
46 T. Xie and I. A. Rousseau, *Polymer*, 2009, **50**, 1852–1856.
47 K. Yu, T. Xie, J. S. Leng, Y. F. Ding and H. J. Qi, *Soft Matter*, 2012, **8**, 5687–5695.